In vitro impedance spectroscopy: A MEA-based measurement bench for myoblasts cultures monitoring

Alexia Bailleul, Julien Claudel, Florence Poulletier de Gannes, Gilles N'kaoua, Florian Kolbl, Fabien Soulier, Noëlle Lewis, Serge Bernard, Sylvie Renaud

In vitro impedance spectroscopy: a MEA-based measurement bench for myoblasts cultures monitoring

Alexia BAILLEUL
IMS, CNRS UMR 5218, Bordeaux INP
Univ. Bordeaux
Talence, France
alexia.bailleul@ims-bordeaux.fr

Julien CLAUDEL
IJL, CNRS UMR 7198
Univ. Lorraine
Nancy, France
julien.claudel@univ-lorraine.fr

Florence POULLETIER DE GANNES
IMS, CNRS UMR 5218, Bordeaux INP
Univ. Bordeaux
Talence, France
florence.poulletier@ims-bordeaux.fr

Gilles N'KAOUA
IMS, CNRS UMR 5218, Bordeaux INP
Univ. Bordeaux
Talence, France
gilles.nkaoua@ims-bordeaux.fr

Florian KOLBL
ETIS, CNRS UMR 8051, ENSEA
Univ. Cergy-Pontoise
Cergy-Pontoise, France
florian.kolbl@ensea.fr

Fabien SOULIER
LIRMM, CNRS UMR 5506
Univ. Montpellier
Montpellier, France
fabien.soulier@lirmm.fr

Noëlle LEWIS
IMS, CNRS UMR 5218, Bordeaux INP
Univ. Bordeaux
Talence, France
noelle.lewis@ims-bordeaux.fr

Serge BERNARD
LIRMM, CNRS UMR 5506
Univ. Montpellier
Montpellier, France
serge.bernard@lirmm.fr

Sylvie RENAUD
IMS, CNRS UMR 5218, Bordeaux INP
Univ. Bordeaux
Talence, France
sylvie.renaud@ims-bordeaux.fr

***Abstract*— Bioimpedance spectroscopy is a promising tool for non-invasive monitoring of tissue structure and fluids. With the objective of using it to assess muscle fatigue in vitro, we have developed a measurement bench allowing the monitoring of myoblasts cultures by bioimpedance measurements. This work presents the setup and its characterization, combining modeling and measurements. This setup relies on a microelectrodes array and a commercial impedance analyzer. Its characterization with Phosphate Buffered Saline is coherent with our simulation. The impedance increases at low frequencies after several cell cultures, due to a degradation of the microelectrode interface. Nevertheless, the measurement bench allows us to detect the presence of myoblasts covering the electrodes in a frequency range from 10 kHz to 100 kHz. The measurement bench is therefore suitable to explore the relative impedance variation as a signature of muscle fatigue.**

Keywords*— *MEA, bioimpedance spectroscopy, cell culture, muscle cells.

I. Introduction

Bioimpedance measurements have recently been investigated to detect changes in muscular tissues, during activity, after an injury or in case of neuromuscular disorders [1-3]. Electrical Impedance Myography (EIM) is of real interest as a clinical diagnosis tool or for the monitoring of muscular fatigue during sportive training. Muscular bioimpedance provides information on the tissue structure and fluids. At the cellular level, where electrical stimulation can be used to simulate muscle fatigue, bioimpedance can also reflect metabolic changes. To our knowledge, the bioimpedance signature of muscle tissue fatigue has not been explored in vitro. We thus developed an experimental bench able to monitor, at the cellular level, myoblasts cultures by bioimpedance measurements.

The bioimpedance frequency spectrum explores a biological tissue at different scales. For instance, bioimpedance spectroscopy is a well-known non-invasive technique for real-time monitoring of various cellular processes (proliferation, toxicity, migration, adherence or remodeling) [4,5].

Bioimpedance measurements rely on electrodes acting as both sensors and actuators. In the case of cultures, electrodes are generally positioned at the bottom of a culture well. We find two main types of electrodes: interdigitated electrodes, consisting of 2 comb-shaped electrodes, and microelectrodes arrays (MEAs) including a large number of electrodes (up to a few thousands). The former allow measurements in only one direction in contrast to the MEAs, which give the possibility to make numerous measurements in different directions in the same culture. MEA technology has been widely used to measure the electrical activity of excitable cells (neurons, cardiomyocytes) [6,7]. MEA devices are classically fabricated with TiN or Pt-deposited electrodes, mostly because of an excellent biocompatibility, although more recent technologies propose poly(3,4-ethylenedioxythiophene, PEDOT) or carbon nanotubes (CNT) deposition to lower the electrode impedance [8]. The use of MEAs to investigate muscle physiology is recent: a few studies present a MEA-based analysis of muscle cells [9-11].

In this context, we built an experimental bench for stimulating C2C12 myotubes while evaluating their fatigue by bioimpedance. The C2C12 cell line is a well-established mouse myoblast cell line, widely used as an in vitro model to study skeletal muscle and the effects of exercise [12,13].

Cellular bioimpedance measurement requires a complete characterization of this MEA bench. This paper presents protocols and results of this characterization and demonstrates the feasibility of bioimpedance measurement with MEA on myoblasts cultures.

This work was supported by the Centre National de la Recherche Scientifique (SMARTSTIM project, CNRS, France) under the PRIME'80 program.

II. Material and Methods

A. Measurement setup

The measurement setup is presented in Fig. 1. It includes a PEDOT-CNT MEA (Multi Channel Systems MCS GmbH, Reutlingen, GE) with an array of 59 PEDOT-covered electrodes of 30µm diameter and 200µm spacing. Impedance measurement is performed by a Keysight E4990A impedance analyzer (Keysight Technologies, Santa Rosa, CA, USA), controlled by a custom Labview™ program. A specific Keysight test fixture is used to characterize liquids (Keysight 16452A liquid test fixture).

To interface the impedance analyzer to the MEA, we designed a custom holder and a PCB. The holder was 3D printed and contains connectors and pogo pins (spring-loaded pins) to access the MEA pads ring. The PCB adapts the four BNC-connectors of the analyzer to a pair of wires that can be plugged into the connectors of the MEA holder. This setup allows us to make measurements on any pair of electrodes by connecting the PCB cables on the pair numbers present on the holder.

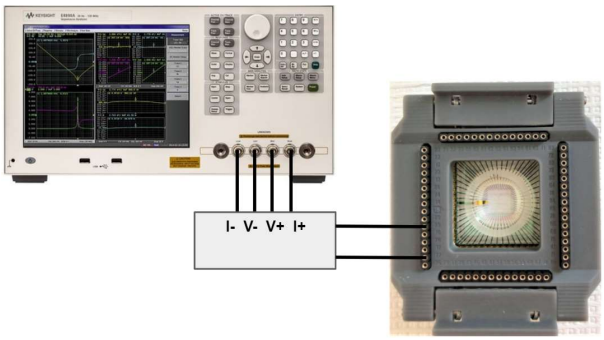

Fig. 1. Illustration of the impedance measurement setup with the analyzer impedance (left), the 3D printed MEA holder (photo on the right) and the symbolized printed circuit board (center).

The setup was used for all impedance measurement experiments. Impedance measurements were performed before cell seeding for characterization purposes, and after cell seeding, when confluence was reached.

Prior to characterization measurements, MEAs were soaked with Phosphate Buffered Saline (PBS) on a heating plate at 30°C for 5h, to increase the hydrophilicity of the electrodes, as recommended by the manufacturer. Then, impedance measurement was performed with MEAs filled with 1 mL of PBS. A 100 mV (pk-pk) sine wave was applied with frequencies ranging from 20 Hz to 10 MHz.

In the case of impedance measurement with seeded cells, MEAs were cleaned with 2.5% tergazyme for at least 2h, dried under the hood and then autoclaved at 121°C for 3 min before cell seeding.

B. Cell culture

For cell culture, C2C12 myoblasts were seeded on MEAs at a density of 200 cells/well. MEAs surface was coated with Matrigel (5% in Dulbecco's Modified Eagle's Medium, DMEM). Cells were cultured with 1 mL of growth medium comprising DMEM supplemented with 10% fetal bovine serum and 1% penicillin-streptomycin. Cells were maintained in an incubator at 37°C under 5% CO_2 atmosphere. The culture media were changed every 48 h.

All products were purchased from Sigma Aldrich, France.

C. Electrical models

To analyze the bioimpedance measurements, we considered electrical models representing the electrical and dielectric properties of the materials involved.

1) Electrode-electrolyte interface

When electrodes are in contact with a saline solution, charge transport phenomena occur at the electrode-electrolyte interface, implying electrons in the electrode material and ions in the electrolyte. These mechanisms are classified into non-faradaic (capacitive) and faradaic effects.

Non-faradaic transport effects appear under the influence of an electric field: ions move towards the electrode-electrolyte interface, and create the so-called ionic double layer as illustrated in Fig. 2(a).

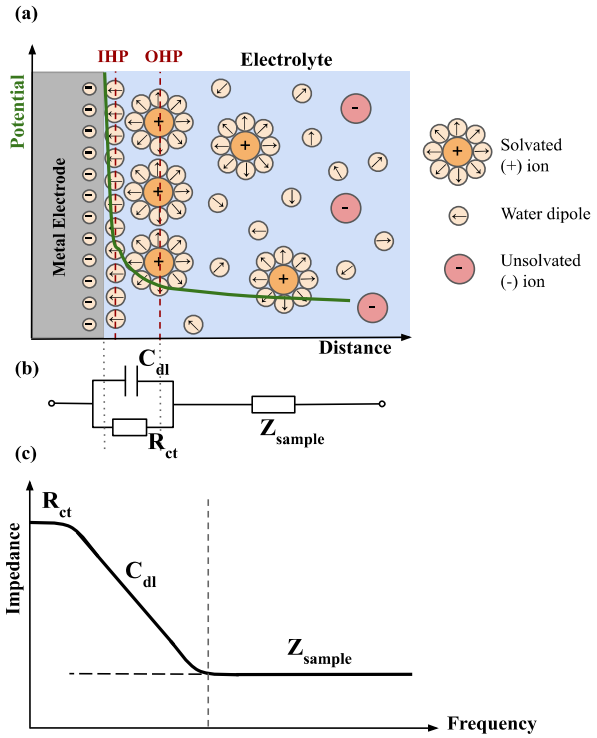

Fig. 2. (a) Electrical double layer at the electrode-electrolyte interface, also called the Helmholtz layer composed of 2 layers: the Inner Helmholtz plane (IHP) and the Outer Helmholtz Plane (OHP), (b) Electrical equivalent circuit of the electrode-electrolyte interface, (c) Impedance spectrum of the electrode-electrolyte interface, underlying the impact of each model component.

The electrical double layer leads to a capacitive effect at Low Frequencies (LF), represented by a capacitance C_{dl} and often masking the characteristics of the electrolyte bulk (Fig. 2(c)). This phenomenon is also known as electrode polarization effect [14].

Faradaic effects consist of a charge transfer across the interface and are represented by an equivalent resistance R_{ct}. Hence, the interface model is classically composed of a double layer capacitance C_{dl} in parallel with a charge transfer resistance R_{ct}, as illustrated in Fig. 2(b).

Actually, charge transfer is a rather undesirable phenomenon in such bioelectronics sensors, as it corresponds to the current generated by redox reactions at the interface. Thus, the excitation signal used for spectroscopy should not reach the very low frequencies, where R_{ct} appears. Then we can neglect R_{ct} as it does not impact the bandwidth of interest of our study.

Finally, the interface impedance depends on the electrode surface:

$$Z_{interface}(\omega) = \frac{1}{j\omega C_{dl}} \quad (1)$$

$$C_{dl} = C_{dl,S}\, S \quad (2)$$

with $C_{dl,S}$ (F/m²) the double layer capacitance per surface area, S (m²) the surface of the electrode.

The double layer capacitance C_{dl} of a solution can be computed from (1) and impedance measurement. Knowing the surface of the electrode, we can quantify the double layer capacitance per surface area with (2).

It is noticeable that the electrodes with a porous material as a top layer present a larger surface area, a phenomenon that is sought with PEDOT deposition treatment.

2) Contribution of electrolyte bulk impedance

In addition to the interface impedance, the electrolyte (or sample under test) contributes in relation to its own electrical and dielectric properties, so that the total impedance can be considered as:

$$Z(\omega) = Z_{sample}(\omega) + Z_{interface}(\omega) \quad (3)$$

If the sample is a pure electrolyte, i.e. an ionic solution, it can be characterized by its conductivity σ_{sol} (S/m) (depending on the ionic concentration) and its relative permittivity $\varepsilon_{r,sol}$. The electrolyte impedance Z_{sample} is then expressed by (4), where K (m^{-1}) is the form factor, depending on the electrode geometry, and ε_0 the vacuum permittivity:

$$Z_{sample}(\omega) = \frac{K}{\sigma_{sol} + j\omega\varepsilon_{r,sol}\varepsilon_0} \quad (4)$$

As a first step, we characterized the solutions we use in our experiments (PBS, culture media): we measured with a dedicated electrode each solution impedance, using the impedance analyzer Keysight E4990A and the Keysight 16452A liquid test fixture.

Intrinsic parameters of a solution (conductivity and permittivity) can be deduced from (4):

$$\sigma_{sol} = \text{real}\left(\frac{K}{Z}\right) \quad (5)$$

$$\epsilon_{r,sol} = \text{imag}\left(\frac{K}{Z}\right)/\omega\epsilon_0 \quad (6)$$

In a second step, we determined the form factor of our MEAs by performing a Finite Element Method (FEM) simulation (Multiphysics® COMSOL AB, Stockholm, Sweden). We simulated 2 microelectrodes of 30 µm diameter and 200 µm spacing, in contact with an homogeneous medium of conductivity (1 S/m). The simulation was performed in direct current assuming a purely resistive medium, without interface effects.

3) Contribution of cellular culture impedance

When the sample consists of a cellular culture, current paths are modified by the adhesion of cells over the electrode surface, as illustrated in Fig. 3(a). The term Z_{sample} is now the impedance of the cellular culture. Parasitic effects coming from the bench itself, especially the parasitic capacitance from connection tracks [15] must be taken into account by using a capacitance C_p.

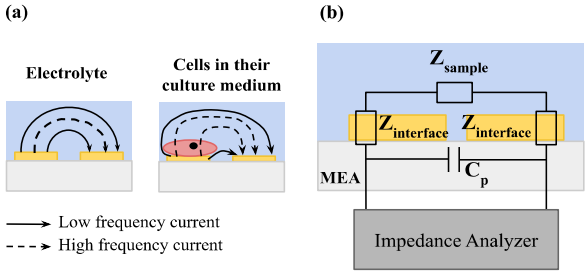

Fig. 3. (a) Effect of cell adhesion on the excitation current, (b) Overall equivalent electrical circuit intervening in each bioimpedance measurement, with Z_{sample} the impedance to measure, $Z_{interface}$ the interface impedance and C_p the parasitic capacitances introduced by the measurement bench and the connection tracks.

The resulting model is displayed in Fig. 3(b). Impedance measurements were performed in a two-point configuration, symmetrically between two electrodes of a MEA. Therefore, the interface effect is doubled as $Z_{interface}$ appears for each electrode in parallel with the parasitic capacitance C_p.

III. Results

A. Electrodes characterization

1) MEAs form factor and theoretical impedance

The first step of the experiment was to determine the intrinsic properties of PBS with a liquid test fixture, which is the solution used for the characterization of MEAs. We measured the PBS impedance and deduced its conductivity, permittivity and C_{dl}. The form factor K of the liquid test fixture was determined by performing a no-load measurement, and using (6). The liquid test fixture surface is 5.67 cm², which with (2) give the double layer capacitance per unit area $C_{dl,S}$. All the intrinsic properties of PBS are summarized in Table I.

TABLE I. Measured parameters of Phosphate Buffered Saline solution

σ_{sol} (S/m)	$\varepsilon_{r,sol}$	$C_{dl,S}$ (µF/cm²)
1.452	78	4.97

The form factor of our microelectrodes was then determined by performing a FEM simulation. The resulting value for K was 30829 m^{-1}.

Finally, using these values and (1), (2) and (4) we simulated the theoretical impedance of our MEAs. Fig. 4 shows the module of the simulated impedance (blue dashed curve). We can see a capacitive behavior at low frequencies up to 1 MHz, and a plateau reaching about 22 kΩ.

The low frequency slope is due to interface effects. We mentioned earlier that these effects depend on the surface of the electrodes, which were considered in the simulation as flat. However, the MEA microelectrodes have a PEDOT

top layer, a porous material that creates a much larger contact area with the sample. Increasing the effective surface (or contact surface) of the electrode decreases the double layer capacitance. This phenomenon is well illustrated in Fig. 4.

We then performed the impedance characterization of our MEA, filled with 1 mL of PBS, in a frequency range from 20 Hz to 10 MHz. Whatever the electrode pair selected for the measurement, results are similar and are plotted in Fig 4 (plain curve). We can observe a capacitive behavior between 20 Hz and 300 Hz, followed by a plateau of about 22 kΩ, and again a capacitive slope starting at 200 kHz.

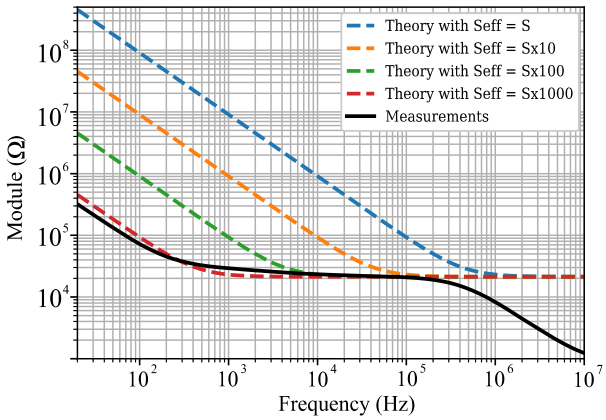

Fig. 4. MEA impedance: measurement vs theoretical impedance with different effective surfaces S_{eff}.

The low frequency slope testifies for interface effects, which disappear at a much lower frequency than expected by the simulation. This is due to the PEDOT porosity of the electrodes, which creates an effective surface 1000 times larger than the surface announced by the manufacturer. This result is consistent with [16] who compared Platinum electrodes and black Platinum electrodes impedance and found an effective surface/geometry area ratio of ~1000.

Both the impedance measurement and the simulated impedance present a plateau of about 22 kΩ, which validates our estimation of the form factor K of the microelectrodes by COMSOL simulation.

Finally, the slope in high frequency can be related, as expected, to the parasitic capacitance from the connection lines and the measurement bench circuitry [15].

According to these results, the region of interest for evaluating the impedance of Z_{sample} is between 300 Hz and 200 kHz.

2) MEA interface degradation

MEAs are fabricated to be re-usable for successive cultures provided that cleaning procedures are respected in between. We characterized the same MEAs from the previous section after their usage for a series of myoblasts cultures (5 cultures), following the same procedure as in the first characterization. Fig. 5 presents the MEA reference impedance before use (black dashed curve, same as in Fig. 4) and the impedance after several usages, plotted for 4 electrode pairs of the same MEA.

After repeated usages, we note an increase of the impedance in the low frequency region. In addition, we note that this increase is not similar for all electrode pairs. We observed this phenomenon on all the MEAs we used, despite our cautious respect of the hydrophilic treatments and cleaning procedures recommended by the manufacturer.

The increase of the impedance at low frequencies suggests a modification of the interface. We hypothesize that the contact area between the electrode and the sample is reduced due to the presence of cellular or coating residues in the PEDOT-CNT nanoporous layer [16,17].

This is an unexpected degradation effect which compromises the analysis of the intrinsic impedance of the cultures, by masking almost entirely the frequency band of interest.

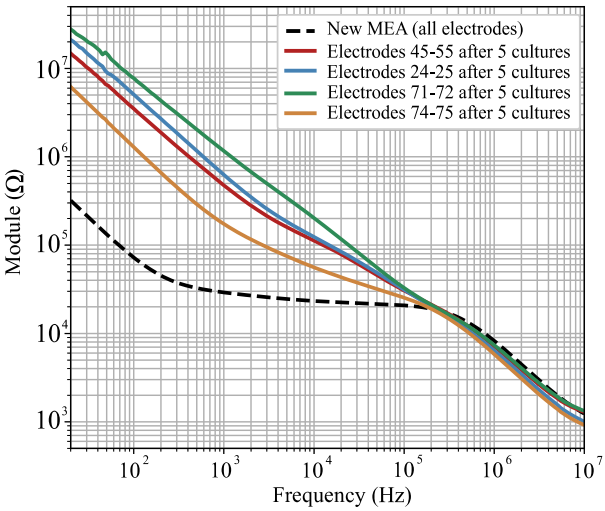

Fig. 5. MEA impedance measured before use, and after repeated usages.

3) Electrical model parameters

To quantify the observed impedance changes before use and after repeated use, we considered a simple electrical model: electrodes interface is modeled by one capacitor C_{dl} (representing $Z_{interface}$ in Fig. 3(b)), in series with a resistor R, considering a purely resistive sample (Z_{sample} in Fig. 3(b)). This RC circuit is in parallel with the parasitic elements, modeled by a capacitor C_p.

At first, we estimated the 3 parameters of the model for an unused MEA. The values extracted from the black dashed curve in Fig. 5 are: C_{dl} = 22.7nF, R = 24kΩ and C_p = 19.9pF. A simulation of this electrical circuit results in an impedance curve as plotted in Fig.6 (dotted curve), to be compared to the measurements (black curve). The model fits our measurements, with a maximum error around 500 Hz corresponding to the transition between the interface impedance and the solution impedance. We attribute the error on the phase at high frequencies to an inductive effect due to the cables present in the measurement bench.

Secondly, we quantified the impedance increase observed after several cultures. As we hypothesize that this increase is related to an interface modification, we consider R and C_p constants. We extracted C_{dl} for each measurement curve (Fig. 5, colored), and simulated the electrical circuit with each C_{dl} value. Fig. 6 shows for the electrode pair 74-75, the impedance measurement and equivalent circuit simulation. On the modulus plot, we can see that our model fits well with

the measurements in low and high frequencies. However, a large difference is noticeable in the central region: the model shows a plateau, corresponding to a resistance-dominated impedance, in contrast to the measurements. Furthermore, we can see that the modulus slope of the measurements at low frequency is not strictly capacitive. On the phase plot, we can observe that the measured phase reaches about 80° instead of 90° in low frequencies, suggesting a Constant Phase Element (CPE) behavior. In addition, we notice again a rise of the measured phase in high frequency, reflecting the inductive effect due to the cables. This phenomenon is not taken into account in our model and can be explained by an insufficient compensation of the connection cables. Finally, in the central region, it clearly appears that the presence of a simple resistor in the model does not reflect the measured behavior. Similar phenomena are observed on plots for other electrode pairs, although, as illustrated by Fig. 5 impedance curves slightly vary with the considered electrodes.

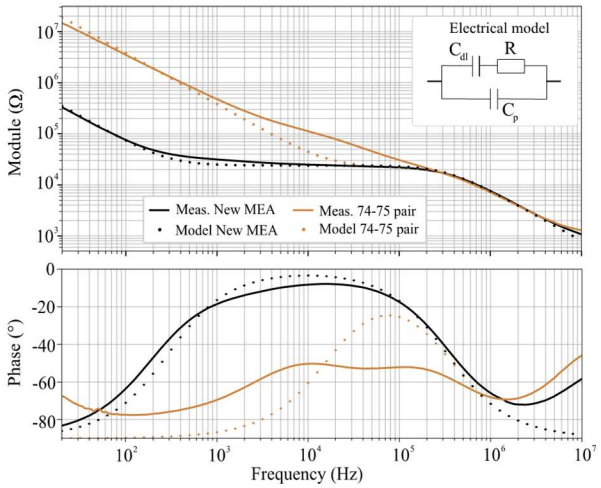

Fig. 6. Impedance characterization on one MEA before use (black, identical for all electrode pairs) and after repeated usages (colored, 74-75 electrode pair): measurement (solid lines) and equivalent electrical model (dotted lines).

These data demonstrate that our model, however simple, provides a good representation of the electrode degradation phenomenon. Nevertheless, the introduction of CPE components in the model will be explored in the future to better interpret the measurements. To characterize this interface degradation, [17] proposed an equivalent electrical model including a resistor and a capacitor in parallel with a CPE in series, explaining that this RC element was necessary due to remaining impurities after the repeated usages of the MEA.

B. Myoblasts detection

While the final objective of our setup is to assess an impedance signature of the muscle cells "fatigue", discriminating between the presence and the absence of cells on microelectrodes is essential for our experimental process. We performed impedance measurement the day before cell seeding, and after the proliferation phase on four PEDOT MEAs. The results for one MEA (9 electrode pairs) are presented in Fig. 7 (top panel). We can see a clear increase of the impedance modulus between 5 kHz and 500 kHz at cellular confluence. We also observe that the standard deviation in the lower frequency is larger, which is consistent with our results (see III.A.2) on the variability of the interface impedance between the different electrodes after several uses.

To identify the most sensitive frequency range for bioimpedance measurement, we computed the normalized relative impedance variation $\Delta|Z|$ over the full frequency range (Fig. 7, bottom panel), using:

$$\Delta|Z| = \frac{|Z|_{cell} - |Z|_{cell\text{-}free}}{|Z|_{cell\text{-}free}} \quad (7)$$

with $|Z|_{cell\text{-}free}$ the impedance before cell seeding and $|Z|_{cell}$ the impedance when confluence was reached.

We can observe that the maximum relative variation occurs between 10 kHz and 100 kHz. This result is consistent with the state-of-the-art, where this frequency range is considered as the region of interest in most bioimpedance studies [1-3,5,18].

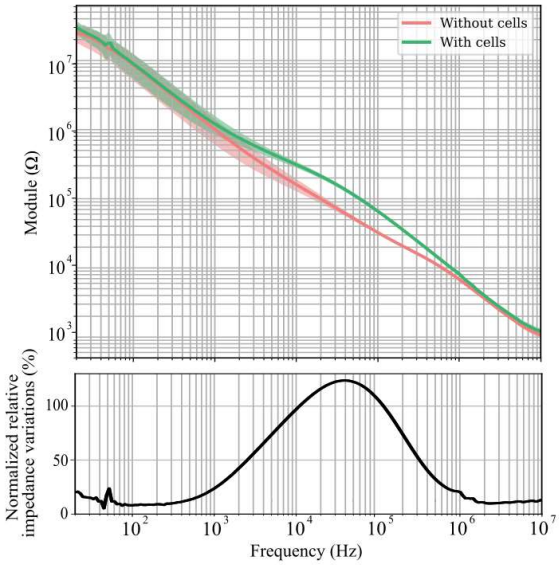

Fig. 7. (top) Mean and standard deviation of the impedance measurements before cell seeding (red) and at confluence (green) (n = 9), (bottom) Relative impedance variations before cell seeding and at confluence.

IV. Conclusion

This work presents a measurement bench dedicated to the monitoring of myoblast cell cultures, by bioimpedance spectroscopy. This bench is intended for the investigation of the bioimpedance signature of muscle cells undergoing metabolic changes, such as fatigue. As a first step, we characterize the setup and demonstrate its sensitivity to muscle cells presence.

The setup main components are a PEDOT-CNT microelectrode array and a commercial impedance analyzer (Keysight E4990A). We simulated the impedance of our bench with a simple electrical model. We then characterized our bench with a MEA filled with PBS solution in the 20 Hz to 10 MHz frequency range and compared the results to the simulation. We found that our model, although simple, provides a good representation of the MEA impedance. In the future, we plan to improve the accuracy of the model by integrating a CPE component. However, our current model remains valid for predicting the useful frequency range of the

bench as it gives an estimation of the frequency from which the interface effects are no longer predominant.

While the MEAs are fabricated to be reusable, we found that the impedance of PEDOT electrodes increases after repeated use, suggesting a degradation of the interface due to an accumulation of impurities in the PEDOT-CNT layer. Taking theses limitations into account, we demonstrated that our measurement bench enables the discrimination between the presence and the absence of muscle cells on electrodes. We identified the frequency region of interest between 10 kHz and 100 kHz, where we observed significant relative impedance variations.

Bioimpedance spectroscopy is a useful tool to study muscle physiology in vitro. Until now, it has been limited to the monitoring of myoblasts differentiation [4, 18] or the assessment of myotubes atrophy and hypertrophy [19]. We have developed a measurement bench to characterize muscle fatigue with bioimpedance measurements: a custom electrical stimulation system is under development to complete the setup. We expect to explore the relative impedance variation as a signature for muscle fatigue when running various stimulation protocols.

ACKNOWLEDGMENT

The authors thank Adrien D'Hollande for his assistance in the experiments.

REFERENCES

[1] B. Fu et T. J. Freeborn, "Biceps tissue bioimpedance changes from isotonic exercise-induced fatigue at different intensities", *Biomed. Phys. Eng. Express*, vol. 4, n° 2, p. 025037, févr. 2018

[2] L. Nescolarde, J. Yanguas, H. Lukaski, X. Alomar, J. Rosell-Ferrer, et G. Rodas, "Effects of muscle injury severity on localized bioimpedance measurements", *Physiol. Meas.*, vol. 36, n° 1, p. 27-42, janv. 2015

[3] Li, J., Jafarpoor, M., Bouxsein, M. and Rutkove, S.B. (2015), "Distinguishing neuromuscular disorders based on the passive electrical material properties of muscle", Muscle Nerve, 51: 49-55

[4] S. M. Murphy, M. Kiely, P. M. Jakeman, P. A. Kiely, et B. P. Carson, "Optimization of an in vitro bioassay to monitor growth and formation of myotubes in real time", *Bioscience Reports*, vol. 36, n° 3, p. e00330, juin 2016

[5] M. R. Cimpan, T. Mordal, J. Schölermann, Z. E. Allouni, U. Pliquett, et E. Cimpan, "An impedance-based high-throughput method for evaluating the cytotoxicity of nanoparticles", *Journal of Physics: Conference Series*, vol. 429, p. 012026, avr. 2013

[6] C. A. Thomas, P. A. Springer, G. E. Loeb, Y. Berwald-Netter, et L. M. Okun, "A miniature microelectrode array to monitor the bioelectric activity of cultured cells", Experimental Cell Research, vol. 74, n° 1, p. 61-66, 1972

[7] M. E. J. Obien, K. Deligkaris, T. Bullmann, D. J. Bakkum, et U. Frey, "Revealing neuronal function through microelectrode array recordings", *Frontiers in Neuroscience*, vol. 8, p. 423, 2015

[8] R. Gerwig *et al.*, "PEDOT–CNT Composite Microelectrodes for Recording and Electrostimulation Applications: Fabrication, Morphology, and Electrical Properties", *Frontiers in Neuroengineering*, vol. 5, p. 8, 2012

[9] C. G. Langhammer, M. K. Kutzing, V. Luo, J. D. Zahn, et B. L. Firestein, "Skeletal myotube integration with planar microelectrode arrays in vitro for spatially selective recording and stimulation: A comparison of neuronal and myotube extracellular action potentials", *Biotechnol Progress*, vol. 27, n° 3, p. 891-895, mai 2011

[10] N. Rabieh, S. M. Ojovan, N. Shmoel, H. Erez, E. Maydan, et M. E. Spira, "On-chip, multisite extracellular and intracellular recordings from primary cultured skeletal myotubes", *Sci Rep*, vol. 6, n° 1, p. 36498, déc. 2016

[11] M. K. Lewandowska, E. Bogatikov, A. R. Hierlemann, et A. R. Punga, "Long-Term High-Density Extracellular Recordings Enable Studies of Muscle Cell Physiology", *Front. Physiol.*, vol. 9, p. 1424, oct. 2018

[12] T. Nedachi, H. Fujita, et M. Kanzaki, "Contractile C $_2$ C $_{12}$ myotube model for studying exercise-inducible responses in skeletal muscle", *American Journal of Physiology-Endocrinology and Metabolism*, vol. 295, n° 5, p. E1191-E1204, nov. 2008

[13] Y. Manabe *et al.*, "Characterization of an Acute Muscle Contraction Model Using Cultured C2C12 Myotubes", *PLoS ONE*, vol. 7, n° 12, p. e52592, déc. 2012

[14] P. B. Ishai, M. S. Talary, A. Caduff, E. Levy, et Y. Feldman, "Electrode polarization in dielectric measurements: a review", *Meas. Sci. Technol.*, vol. 24, n° 10, p. 102001, oct. 2013

[15] A. L. Alves de Araujo, J. Claudel, D. Kourtiche, et M. Nadi, "Influence of Electrode Connection Tracks on Biological Cell Measurements by Impedance Spectroscopy", *Sensors*, vol. 19, n° 13, p. 2839, juin 2019

[16] G. Márton, I. Bakos, Z. Fekete, I. Ulbert, et A. Pongrácz, "Durability of high surface area platinum deposits on microelectrode arrays for acute neural recordings", *J Mater Sci: Mater Med*, vol. 25, n° 3, p. 931-940, mars 2014

[17] D. Krinke, H.-G. Jahnke, O. Pänke, et A. A. Robitzki, "A microelectrode-based sensor for label-free in vitro detection of ischemic effects on cardiomyocytes", *Biosensors and Bioelectronics*, vol. 24, n° 9, p. 2798-2803, mai 2009

[18] I. Park *et al.*, "Electrical Impedance Monitoring of C2C12 Myoblast Differentiation on an Indium Tin Oxide Electrode", *Sensors*, vol. 16, n° 12, p. 2068, déc. 2016

[19] S. Rakhilin *et al.*, "Electrical Impedance as a Novel Biomarker of Myotube Atrophy and Hypertrophy", *Journal of Biomolecular Screening*, vol. 16, n° 6, p. 565-574, juill. 2011